

A Novel Multi-Modal Sensing System Prototype for Cardiovascular and Cardiopulmonary Monitoring

Yusuf Ziya Hayirlioglu and Beren Semiz^a

Department of Electrical and Electronics Engineering, Koc University, Istanbul, Turkey

Keywords: Wearable Devices, Health Monitoring, Seismocardiogram, Photoplethysmogram, Electrocardiogram.

Abstract: Cardiopulmonary disease treatments can highly benefit from remote monitoring systems, allowing for early diagnosis and enabling personalized treatment programs. In this paper, the feasibility and performance of such a system is demonstrated. Continuous and simultaneous monitoring of electrocardiogram (ECG), seismocardiogram (SCG), photoplethysmogram (PPG), and body temperature signals from a total of six sensors is achieved by a microcontroller-based setup, which consists of a fixed main body mounted on mid-sternum and a mobile daughter body mounted on the wrist. The data is stored in an SD card and transmitted by a Bluetooth to PC in real-time, allowing easy data access. The proposed system's performance is examined in comparison to the heart rate (HR), heart rate variability (HRV), and respiration rate metrics derived from the BIOPAC system's ECG and respiration data. Low margins of error in all test cases show that the system works at high performance.

1 INTRODUCTION

According to the 2020 report of the World Health Organization, cardiopulmonary diseases are among the leading causes of death, constituting a significant fraction of the total deaths worldwide (~30%) (WHO, 2020). In addition, Hospital Readmissions Reduction Program (2010), which was passed under the Affordable Care Act, reported heart failure, acute myocardial infarction and pneumonia as the top three health problems that should be focused on to reduce re-hospitalization rates (Zuckerman et al., 2016). Considering these facts, remote and continuous monitoring systems could potentially allow early diagnosis and intervention, enable the generation of personalized treatment programs, and provide proactive and preventive treatment protocols for individuals at risk of cardiovascular and cardiopulmonary diseases (Sana et al., 2020).

The main methods used in the clinic for diagnosis and follow-up can be listed as assessing (i) the vital signs (blood pressure, heart rhythm, respiratory rhythm, body temperature), (ii) chest and lung sounds, (iii) heart sounds, and (iv) vascular health (Gupta and Shea, 2021). Hence, there is a compelling need for novel sensing modalities and anal-

ysis pipelines to digitize these examination steps and to achieve continuous health monitoring regardless of time and environmental stressors.

Since the electrical, mechanical, acoustic and optical signals recorded from the human body have physiological origins, they can provide clinically useful information about the underlying anatomical and physiological conditions. Among the aforementioned signals, the most commonly used ones are the electrocardiogram (ECG), seismocardiogram (SCG) and photoplethysmogram (PPG) waveforms. While the ECG measures the electrical activity of the heart, the SCG assesses the mechanical activity originating from the contraction of the heart and ejection of blood from the ventricles (Inan et al., 2014). Studies have shown that the SCG signal can be leveraged in estimating systolic time intervals (Shandhi et al., 2019), assessment of myocardial contraction (Tavakolian et al., 2012), heart failure classification (Inan et al., 2018), studying respiration rate and phases (Pandia et al., 2012), and derivation of hemodynamic parameters such as stroke volume (Semiz et al., 2020). On the other hand, the PPG is generated as a result of the variance in the amount of light absorbed in the arteries due to the changes in arterial blood volume during the cardiac cycle. In the literature, it has been shown that analysis of the PPG signal can provide important information regarding

^a  <https://orcid.org/0000-0002-7544-5974>

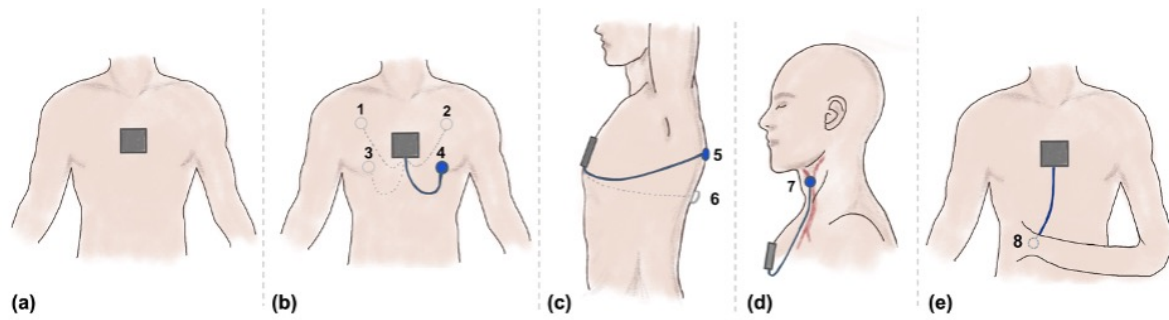


Figure 1: (a) The main body of the proposed wearable device was designed in such a way that ECG, SCG, PPG and body temperature measurements could be taken continuously. (b-e) The removable daughter body was planned to be designed to allow additional SCG and PPG measurements to assist in the analysis.

blood oxygen level, blood pressure and vascular resistance assessment (cheol Jeong et al., 2018).

Although there are several wearable system prototypes utilizing ECG, SCG and PPG signals separately in the literature (Fattah et al., 2017; Li et al., 2017; Di Rienzo et al., 2011; Hernandez et al., 2014; Da He et al., 2011), they have generally been limited to focusing on heart rhythm assessment. Thus, none of them allows comprehensive cardiovascular and cardiopulmonary monitoring as the aforementioned examination steps could not be digitized altogether. On the other hand, systems allowing multiple measurements only enable the recording of signals from the location where the device is attached, thus cannot provide any mobility function (Etemadi et al., 2015). Since such a system is also expected to evaluate lung health, respiratory and blood pressure parameters, having an adaptable and mobile system is crucial. In addition to all these, it is necessary to develop a system that allows real-time data transfer to enable timely intervention.

In this paper, for the first time to the best of our knowledge, an adaptable wearable patch prototype is designed to enable (i) comprehensive cardiovascular and cardiopulmonary monitoring through simultaneous acquisition of various physiological signals (ECG, SCG, PPG and body temperature). The proposed design includes a main body to be mounted on the mid-sternum and a removable daughter body to allow additional SCG and PPG measurements to assist in comprehensive cardiopulmonary and cardiovascular assessment (Fig. 1). The proposed prototype (ii) supports both real-time data transfer and SDcard recording, is (iii) developable and adaptable. Once improved and converted into printed-circuit-board (PCB) form, the system will be (iv) mobile, thus will be convenient for the patients and healthcare professionals for use in various environments, both inside and outside clinic.

2 METHODS

2.1 Hardware

As previously mentioned, the long-term aim is to develop a PCB-based multi-modal wearable system, which would consist of the following two parts:

- **MAIN BODY** to be mounted on the chest, which houses the sensors for measuring the body temperature, ECG, proximal PPG and SCG signals, the microcontroller to which all sensors will be connected, the battery of the system, and the Bluetooth and microSD card modules (Fig. 1(a)).
- **DAUGHTER BODY** to be mounted on distal locations, which houses the sensors that can be attached or detached from the main body and allows recording of distal SCG and PPG signals (Fig. 1(b-e)).

Based on this design, in this paper, a development-kit-based system prototype is presented (Fig. 2(a)). First, the sensors in the market and literature were investigated and the most suitable ones were determined.

2.1.1 Seismocardiogram (SCG) and Photoplethysmogram (PPG)

In the literature, analysis of the SCG signal has generally been performed at <100 Hz frequency values and it has been shown that having a sample rate around 500 Hz is sufficient (Semiz et al., 2020). Although analog accelerometers have higher bandwidth compared to digital accelerometers, the main aim was to select an accelerometer having low noise, high resolution, and sensitivity to allow measurement of peak-to-peak amplitude values within the limits of <10 mg. Hence, it was decided to use the ADXL355 (Analog Devices, Norwood, MA, USA) accelerometer with $25 \mu\text{g}/\sqrt{\text{Hz}}$ noise floor and 0.003 mV/bit resolution,

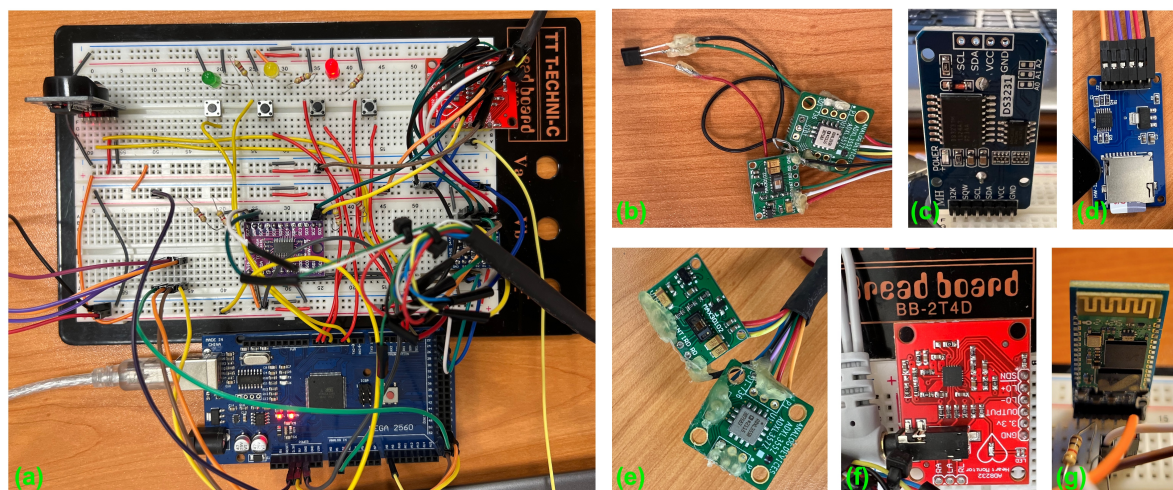


Figure 2: (a) General view of the system, (b) Temperature, MAX30102 and ADXL355 sensors to be mounted on the chest area, (c) DS3231 RTC module, (d) HW-125 microSD card module, (e) MAX30102 and ADXL355 sensors to be mounted on the wrist area, (f) AD8232 analog front-end IC, (g) HC-05 Bluetooth module.

which has been proven successful in previous studies (Ganti et al., 2020). In accordance with the design, two ADXL355 accelerometers were included in the system, one for each of the main (chest) and daughter bodies (Fig. 2(b) and (e)).

For the PPG signal, first the systems available in the market were examined. Smart watches on the market mostly rely on the use of green light emitting diode (LED) as green LED has relatively higher signal quality and is less susceptible to motion artifacts compared to red and infrared lights. However, green LED-based systems could only allow the measurement of the microvascular network on the skin surface due to green light's relatively lower wavelength. On the contrary, red and infrared lights have longer wavelengths, thus can penetrate into the depths where the arteries are located in the tissue (Lee et al., 2013; Maeda et al., 2011). Hence, in the design of the PPG system, the use of red and infrared LEDs was preferred. To this end, a digital MAX30102 (Maxim Integrated, Sunnyvale, CA, USA) sensor with a resolution of 0.05 mV/bit and a sampling rate of 3200 samples/second has been deemed appropriate. Two MAX30102 sensors were included in the system, one for the main (chest) and one for the daughter body (Fig. 2(b) and (e)). It should be noted that MAX30102 only has one I2C address, therefore, an I2C multiplexer, TCA9548A (Texas Instruments, Dallas, TX, USA), was used to prevent any communication conflict when utilizing two of them.

While the ADXL355 and MAX30102 sensors both support I2C communication, the maximum clock frequency ADXL355 supports is 3.4 MHz, and the maximum clock frequency MAX30102 supports

is 400 kHz. Therefore, the maximum clock frequency of the I2C protocol would be 400 kHz when the same signal bus is used. 400 kHz was deemed to be sufficient considering the requirements of the prototype. Additionally, the ADXL355 is a 3 V sensor with no on-board regulators and the current prototype runs with 5 V. To prevent any damage to the sensor, we used logic level enhancement mode field effect transistors, BSS138 (ON Semiconductor Corporation, Phoenix, Arizona, USA), in the I2C bus. Both ADXL355 and MAX30102 packages include built-in FIFOs, allowing temporary storage of data.

2.1.2 Electrocardiogram (ECG) and Body Temperature

To record the ECG signal, AD8232 (Analog Devices, Norwood, MA, USA) analog front-end integrated circuit (IC) with a noise floor of $100 \text{ nV}/\sqrt{\text{Hz}}$, gain of 100, and gain-bandwidth product of 100 kHz was selected (Fig. 2(f)). Three gel electrodes were mounted in the Einthoven's triangle arrangement and the signals obtained through these electrodes were conditioned by AD8232. The resulting signal was then sampled at 10 bit resolution and 500 Hz by ATMEGA2560's analog-to-digital converter (ADC).

For body temperature measurement, LM35 (Texas Instruments, Dallas, TX, USA) analog IC with $\pm 0.5^\circ\text{C}$ accuracy, $10 \text{ mV}/^\circ\text{C}$ linear scale factor, -55°C - 150°C measurement range and $600 \text{ nV}/\sqrt{\text{Hz}}$ noise floor was chosen and integrated into the part to be mounted on the chest (Fig. 2(b)). The signal was sampled by the ATMEGA2560's ADC at 10-bit resolution and 1 Hz.

2.1.3 Microcontroller

The features considered in the selection of the microcontroller were as follows: having enough processing power to collect data at the desired sampling rates, working with as low power as possible, having a high storage area and EEPROM, and having a sufficient number of analog and digital pins. With 256 KByte memory, 8 KByte EEPROM, 16 analog pins, and 86 programmable input/output lines, AT-MEGA2560 was deemed sufficient for the prototype. Powered at 5 V in active mode with an 11.0592 MHz crystal oscillator, it has a current consumption of 14 mA, and a current consumption of 0.1 μ A in power-off mode. Having four 16-bit timers and six hardware interrupts also had a positive effect on the microcontroller choice.

2.1.4 Data Storage and Transfer

To achieve real-time data transfer, Bluetooth functionality was included in the prototype. In addition to Bluetooth connection, data is simultaneously saved on the microSD card to act as a back-up. For the SD card a high write speed is desired for faster operation. The SD card of choice was a 16GB SanDisk Ultra with an 80 MB/s write speed. The SD card was integrated into the system through HW-125 microSD card module (Fig. 2(d)) and file naming was provided by the date/time stamps taken from the DS3231 RTC module (Fig. 2(c)).

For Bluetooth connection, HC-05, which has a maximum baud rate of 1328400 and can work as both slave and master, was selected (Fig. 2(g)). In the system, 24 KBytes of data was produced per second, while the Bluetooth could reach a data transmission rate of 132 KBytes per second. While searching for a device to be connected, the query time interval, query time, paging time interval and paging time were set as 640 ms, 0.625 ms, 640 ms, and 0.625 ms, respectively to ensure that the Bluetooth consumes less power than it does with its default parameter values. When connected to a device, the Bluetooth was put into sniff mode, so that it consumes less power while waiting for a command during communication. The maximum time, minimum time, test time and waiting time for the sniff mode were selected as 125 ms, 6.25 ms, 1.25 ms, and 5 s, respectively.

It should be noted that when the data is being stored and transferred, all data points are processed simultaneously due to data structure to be used. Although not all sensors are sampled at 500 Hz, all data is stored and transferred at the highest sampling rate. Therefore signals with sampling rates smaller than 500 Hz will have repeating samples in them.

2.2 Firmware

First, the time required to read data from the sensors, save it on the SD card, and send it via Bluetooth while the system reaches the desired sampling rates was investigated. I2C communication was established at the clock frequency of 400 kHz, due to MAX30102's speed constraint. With this communication speed, samples could be read from both infrared and red LEDs of the MAX30102 at approximately 0.9 ms, and the X, Y and Z axes of ADXL355 at 0.6 ms. And for the analog data, it took around 0.15 ms to read one sample. Overall, two MAX30102s, two ADXL355s, one ECG and one temperature sensor were included in the system. The ADXL355 and MAX30102 collect data at 500 Hz and 200 Hz sample rates respectively. The data MAX30102 collects is subjected to an on-chip sample averaging operation, leading to an effective sampling rate of 50 Hz. The ECG is sampled at 500 Hz and the temperature sensor is sampled at 1 Hz.

Based on these specifications, reading data from the accelerometers (0.6 ms each) and the ECG sensor (0.15 ms) were taking 1.35 ms of a 2 ms cycle. When various other operations were added into the system (e.g., writing data to SD card, sending data over Bluetooth, reading data from MAX30102), it was observed that data could not be timely obtained from the sensors which required to be sampled at 500 Hz, resulting in data skipping when the FIFOs overflow. To overcome this problem, an algorithm was developed. In this algorithm, the time spent by AT-MEGA2560 in the statements was calculated. The primary timer-controlled statement, which executes most frequently, needs to be completed in less than 2 ms due to 500 Hz sampling rate requirement. If the microcontroller goes over 2 ms in the statement, the extra time spent is stored in a variable and is incremented with each occurrence of such an event. In the case when the extra time it calculates goes over 2 ms, the microcontroller is forced to read from FIFOs of the sensors and the virtual FIFO created for the ECG. With this algorithm, it was ensured that the microcontroller will collect all available data from the sensors without missing any samples.

The reasoning behind using a virtual FIFO for the ECG is because the ECG samples were not being collected at constant intervals due to variable statement execution times, causing both data skipping and data shifting. By using the FIFOs of the MAX30102 and ADXL355, the data could be collected at the desired frequencies without any data shift and with the help of the aforementioned algorithm, data skipping problem was also solved. However, the analog ECG sensor,

which lacks any kind of storage element, was experiencing data skipping and small data shifts. As a solution, a virtual FIFO and timer interrupts were used. Whenever data needs to be read from the ECG sensor, the ATMEGA2560 is interrupted by the timer and a data point is sampled from the ECG sensor. This ensures that the ECG is sampled at constant intervals. The sample is then stored in the virtual buffer created for the ECG until it is written to the SD card and transmitted by the Bluetooth.

Four different modes (*Start Recording*, *Pause Recording*, *Stop Recording* and *Low Power*) have been added to the system via buttons using hardware interrupts to control recording capability and power consumption. In *Start Recording* mode, the system starts reading data by creating a new file on the SD-card and writes the data it reads to this file. The name of the file is determined by the timestamp captured by the DS3231 RTC module. *Pause Recording* mode temporarily stops recording while recording is in progress, but does not close the file. To continue recording, *Pause Recording* button should be pressed again. In *Stop Recording* mode, the created file is closed and recording is stopped. Data written to the SDcard is simultaneously sent to Bluetooth via the serial port and to PC via Bluetooth. To test the Bluetooth connection with a PC, PuTTY was used. The data that PuTTY writes to its console is saved in a log file. The last mode, *Low Power* mode turns off the sensors and communication channels busses on the system, and puts the microcontroller in low power mode, minimizing power consumption.

2.3 Data Collection Protocol

This study was conducted under a protocol approved by the Koc University Institutional Review Board and all subjects provided written consent. The system was tested on two subjects (one male and one female) with no history of cardiovascular or cardiorespiratory diseases. The main body of the system (Fig. 2(b)) including a tri-axial accelerometer, PPG module and temperature sensor was mounted on the mid-sternum of the subject using hypoallergenic transparent medical tape. Three ECG cables were attached to the chest through gel electrodes in accordance with Einthoven’s triangle. Additionally, the daughter body (Fig. 2(e)) including a tri-axial accelerometer and PPG module was placed on the wrist with the same medical tape. It should be noted that the accurate direction of the accelerometers and skin-contact of PPG sensors were ensured before starting data collection.

Along with the signals collected through the prototype, reference respiration and ECG signals were

recorded simultaneously with the BIOPAC system (BIOPAC Systems, Inc. Goleta, CA, USA). Reference respiration signal was measured using respiration effort transducer and reference ECG signal was acquired through three gel electrodes. The signals were transferred to the BIOPAC system using wireless Bionomadix RSPEC-R module (BIOPAC Systems, Inc. Goleta, CA, USA). All reference signals were sampled at 500 Hz.

As the main goal was to validate the system, the protocol did not include any physiological modulation. Instead, the subjects stood motionless vertically for five minutes. The signals were post-processed using MATLAB (MathWorks, Natick, MA, USA).

2.4 Data Analysis

In this section, physiological parameters derived from the reference signals and the ones acquired with the prototype were compared to assess the performance of the prototype. First, the signals were filtered using digital finite impulse response (FIR) band-pass filters in accordance with the bandwidths reported in the literature (Carek et al., 2017; Pandia et al., 2012; Shandhi et al., 2019). For ECG and PPG, frequency ranges were determined as 0.5 - 40 Hz and 1 - 16 Hz, respectively. For the SCG signals, two different FIR filters were implemented. The one having 0 - 1 Hz range, which corresponds to the chest movements originating from exhalation and inhalation, was applied to derive the respiratory information. On the other hand, the one having 1- 40 Hz bandwidth was used to represent the vibration and acoustic information originating from the cardiac output and heart sounds.

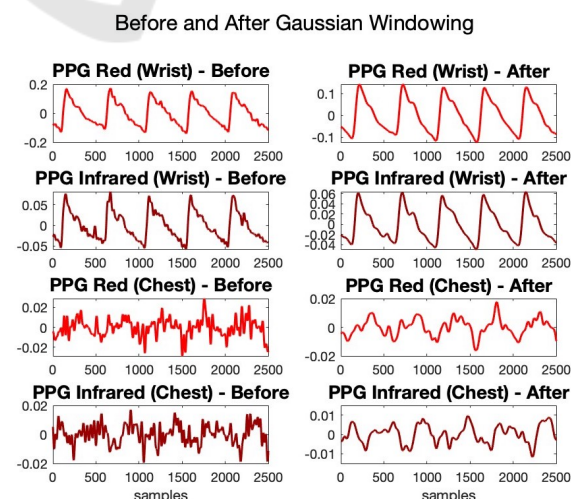


Figure 3: PPG signals before and after Gaussian windowing.

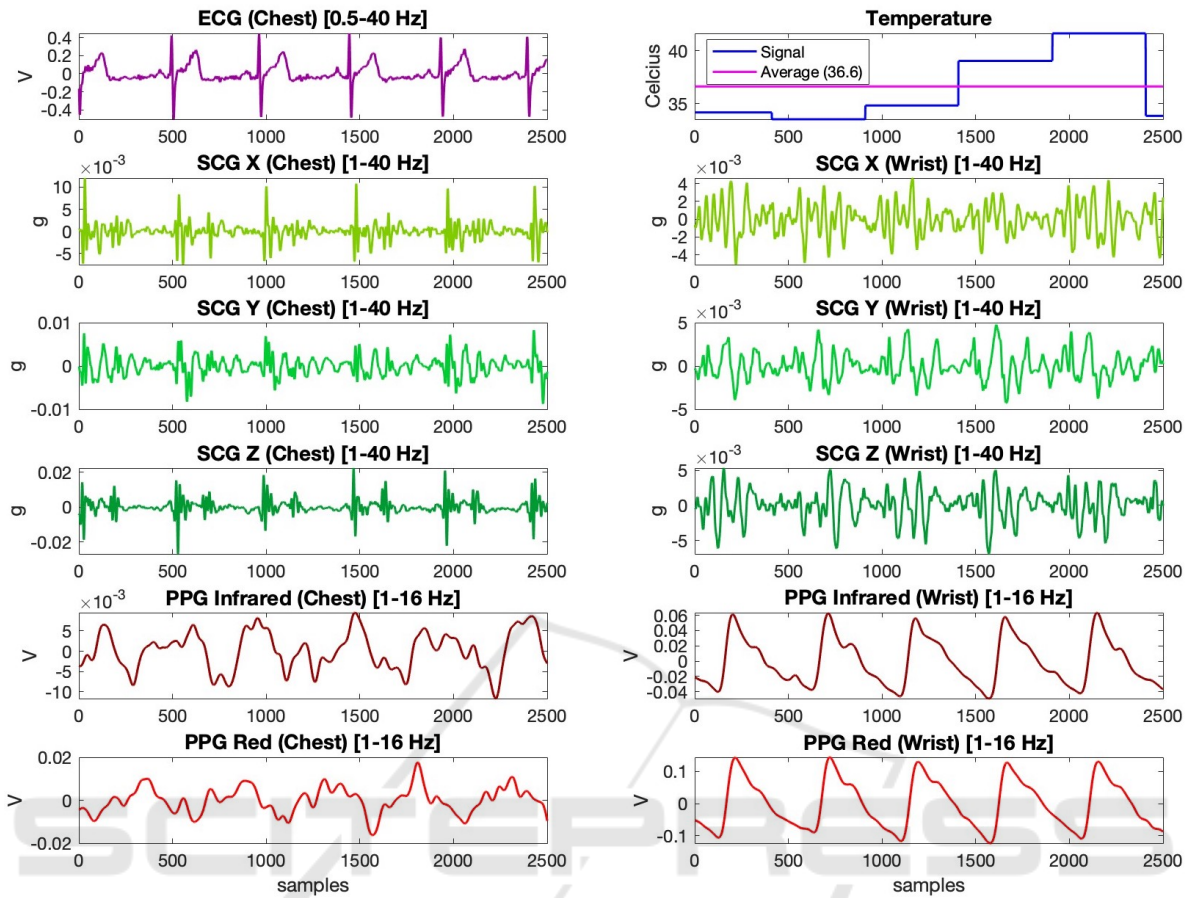


Figure 4: 5-second-long, pre-processed segments of the signals acquired with the system.

2.4.1 Derivation of Heart Rate and Heart Rate Variability

First, performance of the prototype in estimating heart rate (HR) and heart rate variability (HRV) values through the acquired ECG and PPG signals was assessed. It has been observed that the PPG signals taken from the chest in particular contain a high level of noise, therefore it was more difficult to determine the peak and diastolic points compared to the PPG taken from the wrist. This was an expected result, as it was more difficult to reach the microvascular region in the chest area compared to the wrist. To mitigate the negative impact of signal quality, Gaussian smoothing (window length: 100, width factor: 2.75) was applied to smooth out these noise-based oscillations observed in the signals. 5-second-long segments from the PPG signals before and after Gaussian windowing were presented in Fig. 3. HR and HRV were then calculated using the following steps:

1. First, reference HR and HRV values were calculated using the reference ECG signal recorded with the BIOPAC system. To this end, R-points on

the ECG were determined and an **RR** vector was created by calculating intervals between successive R-points. HR in beats per minute (bpm) and HRV in milliseconds were calculated on this vector using Eq. 1 and Eq. 2, respectively (*std*: standard deviation, F_s : sampling rate). The standard deviation of inter-beat-interval (SDNN) is measured in ms. The short-term recording for SDNN is 5 minutes (Shaffer and Ginsberg, 2017).

2. After computing the reference values, HR and HRV were derived from the ECG signal acquired through the prototype using the same formulas.
3. In the last step, PPG signals acquired through the prototype from the wrist and chest were used to derive the HR and HRV values. By calculating the time interval between consecutive peaks on the Gaussian-windowed red and infrared PPG signals, a **PP** vector similar to the **RR** vector was generated. HR and HRV values were calculated using the same formulas, but inserting the **PP** vector instead of the **RR** vector.
4. To calculate the percent error (*%error*), Eq. 3

Table 1: Heart rate and heart rate variability calculations (bpm: beats per minute, ms: milliseconds).

First Subject				
	Heart Rate (bpm)	Error (%)	Heart Rate Variability (ms)	Error (%)
BIOPAC ECG (Reference)	65.2	-	15.2	-
Wearable ECG	65.9	1.07	15.9	4.61
Wearable PPG Infrared (Wrist)	65.6	0.61	15.3	0.66
Wearable PPG Red (Wrist)	65.6	0.61	15.3	0.66
Wearable PPG Infrared (Chest)	66.3	1.68	15.5	1.97
Wearable PPG Red (Chest)	67.2	3.07	15.7	3.29
Second Subject				
BIOPAC ECG (Reference)	88.8	-	15.0	-
Wearable ECG	90.2	1.58	17.2	14.6
Wearable PPG Infrared (Wrist)	90.2	1.58	17.2	14.6
Wearable PPG Red (Wrist)	89.8	1.12	17.2	14.6
Wearable PPG Infrared (Chest)	88.9	0.11	17.2	14.6
Wearable PPG Red (Chest)	91.9	3.49	17.4	16.0

was used where *actual* stands for the reference HR and HRV values and *calculated* stands for the ones computed using the ECG, PPG-red and PPG-infrared signals acquired from the prototype.

$$HR = \frac{60 * F_s}{\text{mean}(\mathbf{RR})} \quad (1)$$

$$HRV = \frac{F_s}{\text{std}(\mathbf{RR})} * 1000 \quad (2)$$

$$\%error = \frac{\text{actual} - \text{calculated}}{\text{actual}} * 100 \quad (3)$$

2.4.2 Derivation of Respiration Rate

SCG signal, which was filtered in 0 - 1 Hz range, was used to extract respiratory information. The analysis was specifically performed on the dorso-ventral axis in accordance with the literature (Pandia et al., 2012). Subsequently, Gaussian windowing was applied as previously done in PPG case to smooth out the oscillations observed in the signal. Using the peaks on these signals, reference and SCG-derived respiration rates (number of exhalation-inhalations in one minute) were calculated.

3 RESULTS AND DISCUSSION

3.1 System Performance

5-second-long, pre-processed segments of the signals acquired with the system from one of the subjects were presented in Fig. 4. As can be seen from the plots, the sensors could successfully collect the physiological signals at the desired sampling rates. In addition, the representative SCG signals written to SD

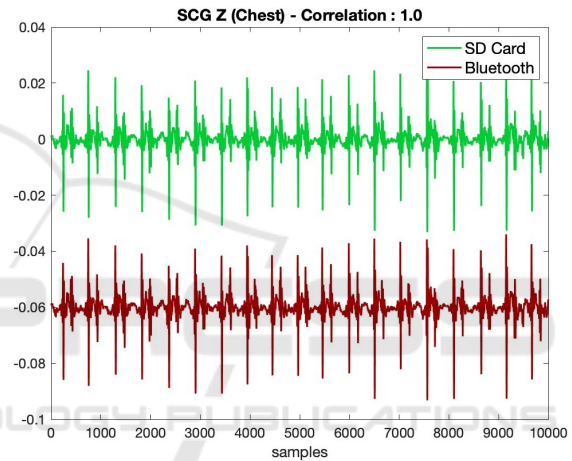


Figure 5: Comparison of representative SCG signals written to SD card and transferred to computer via Bluetooth. There was a correlation of 100% and no data loss was observed during Bluetooth transmission.

card and transferred to computer via Bluetooth are presented in Fig. 5. It should be noted that the signal received via Bluetooth has been shifted down in the y-axis to facilitate visualization. As seen, there is a 100% correlation between the signals and there is no data loss during transmission via Bluetooth.

3.2 Comparison with Reference Measurements

3.2.1 Heart Rate and Heart Rate Variability

First, the performance of the prototype in estimating HR and HRV values through the acquired ECG and PPG signals was assessed. As detailed in Section 2.4.1, HR and HRV were calculated using the time intervals between the consecutive peak locations on ECG and PPG signals. On the other hand, the ref-

Table 2: Breathing Rate Calculations (breaths per minute).

	First Subject	Error (%)	Second Subject	Error (%)
BIOPAC Belt (Reference)	24.5	-	21.1	-
Wearable SCG-Z (Chest, 0-1 Hz)	24.8	1.22	20.7	1.89

erence HR and HRV were calculated using the peak locations on the ECG acquired with the BIOPAC system. The resulting HR and HRV values for both subjects are presented in Table 1. The low margin of error between the reference and prototype-derived values shows the high performance of the designed system. Specifically, there is a maximum of 2-beat difference between the reference HR values and the ones derived from ECG and PPG signals acquired from chest and wrist. Additionally, although the PPG signal qualities obtained from the chest and wrist were different (chest being more susceptible to artifacts), this negative effect could be eliminated with filtering and Gaussian smoothing. Indeed, the HR values obtained from the chest and wrist resulted in negligible errors, both being similar to the reference HR measurements.

3.2.2 Respiration Rate

20-second-long segments from the reference and SCG-derived respiration signals from one of the subjects were presented in Fig. 6. As seen in the figure, the respiratory signal generated from the SCG signal moves in parallel with the reference respiratory signal. In addition, the number of breaths per minute calculated on the reference and SCG signals for both subjects is presented in Table 2. For the first subject, reference and SCG-based breathing rates were calculated as 24.5 and 24.8 breaths per minute, respectively. For the second subject, these values were 21.1 and 20.7, respectively. Obtaining almost the same number of respiration cycles with the reference waveform in both subjects shows that the sensors in the system and the signal improvement methods work at high performance.

4 CONCLUSIONS

In this work, an adaptable wearable patch prototype is designed to enable comprehensive cardiovascular and cardiopulmonary monitoring through simultaneous acquisition of ECG, PPG, SCG, and body temperature signals. The design includes a main body to be mounted on the mid-sternum to collect proximal ECG, SCG, PPG and body temperature signals, and a removable daughter body to allow distal SCG and

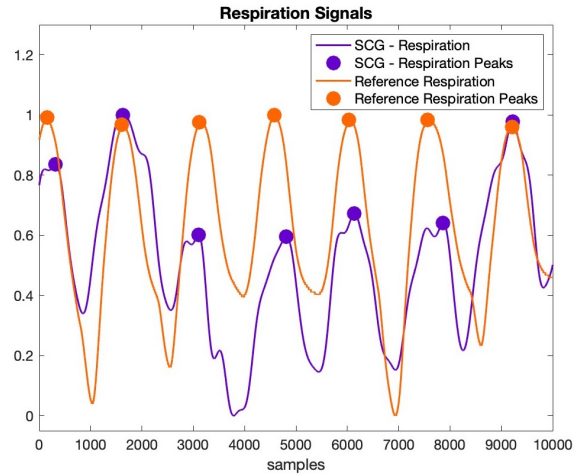


Figure 6: Comparison of the reference and SCG-derived respiratory signals.

PPG measurements to assist in comprehensive health assessment. Respiration rate, HR and HRV values from two subjects obtained from the prototype were compared with the reference ones acquired with the BIOPAC system. Obtaining a low margin of error in all cases showed that the prototype and the signal improvement methods work at high performance. In addition, the signals transferred with the Bluetooth system achieved 100% correlation with the signals saved on the SDcard. Despite receiving data from so many sensors, having no data loss was indeed a promising result for the future versions of the current prototype.

Future work will focus on validating the system with a larger dataset including subjects having varying physiological and demographic features. Additionally, since the calculation of oxygen saturation and blood pressure values from the PPG signal primarily requires a calibration step, studies in this area will be carried out after collecting data from a large number of participants. In the long run, the prototype will be converted into the PCB form having actual main and daughter bodies to allow cable-free measurements. Such a system will potentially be convenient for the patients and healthcare professionals to achieve continuous health monitoring regardless of time and environmental stressors.

ACKNOWLEDGEMENTS

This work was supported by the Scientific and Technological Research Council of Turkey (TUBITAK) under grant number 121E133.

REFERENCES

- Carek, A. M., Conant, J., Joshi, A., Kang, H., and Inan, O. T. (2017). Seismowatch: wearable cuffless blood pressure monitoring using pulse transit time. *Proceedings of the ACM on interactive, mobile, wearable and ubiquitous technologies*, 1(3):1–16.
- cheol Jeong, I., Bychkov, D., and Searson, P. C. (2018). Wearable devices for precision medicine and health state monitoring. *IEEE Transactions on Biomedical Engineering*, 66(5):1242–1258.
- Da He, D., Winokur, E. S., and Sodini, C. G. (2011). A continuous, wearable, and wireless heart monitor using head ballistocardiogram (bcg) and head electrocardiogram (ecg). In *2011 Annual International Conference of the IEEE engineering in medicine and biology society*, pages 4729–4732. IEEE.
- Di Rienzo, M., Meriggi, P., Rizzo, F., Vaini, E., Faini, A., Merati, G., Parati, G., and Castiglioni, P. (2011). A wearable system for the seismocardiogram assessment in daily life conditions. In *2011 Annual International Conference of the IEEE Engineering in Medicine and Biology Society*, pages 4263–4266. IEEE.
- Etemadi, M., Inan, O. T., Heller, J. A., Hersek, S., Klein, L., and Roy, S. (2015). A wearable patch to enable long-term monitoring of environmental, activity and hemodynamics variables. *IEEE transactions on biomedical circuits and systems*, 10(2):280–288.
- Fattah, S. A., Rahman, M. M., Mustakin, N., Islam, M. T., Khan, A. I., and Shahnaz, C. (2017). Wrist-card: Ppg sensor based wrist wearable unit for low cost personalized cardio healthcare system. In *2017 IEEE Global Humanitarian Technology Conference (GHTC)*, pages 1–7. IEEE.
- Ganti, V. G., Carek, A. M., Nevius, B. N., Heller, J. A., Etemadi, M., and Inan, O. T. (2020). Wearable cuffless blood pressure estimation at home via pulse transit time. *IEEE Journal of Biomedical and Health Informatics*, 25(6):1926–1937.
- Gupta, J. and Shea, M. (2021). Cardiovascular examination. *Merck Manual*. [https://www.merckmanuals.com/en-pr/professional/cardiovascular-disorders/approach-to-the-cardiac-patient/cardiovascular-examination\(visited:2022-09\)](https://www.merckmanuals.com/en-pr/professional/cardiovascular-disorders/approach-to-the-cardiac-patient/cardiovascular-examination(visited:2022-09)).
- Hernandez, J., Li, Y., Rehg, J. M., and Picard, R. W. (2014). Bioglass: Physiological parameter estimation using a head-mounted wearable device. In *2014 4th International Conference on Wireless Mobile Communication and Healthcare-Transforming Healthcare Through Innovations in Mobile and Wireless Technologies (MOBIHEALTH)*, pages 55–58. IEEE.
- Inan, O. T., Baran Pouyan, M., Javaid, A. Q., Dowling, S., Etemadi, M., Dorier, A., Heller, J. A., Bicen, A. O., Roy, S., De Marco, T., et al. (2018). Novel wearable seismocardiography and machine learning algorithms can assess clinical status of heart failure patients. *Circulation: Heart Failure*, 11(1):e004313.
- Inan, O. T., Migeotte, P.-F., Park, K.-S., Etemadi, M., Tavakolian, K., Casanella, R., Zanetti, J., Tank, J., Funtova, I., Prisk, G. K., et al. (2014). Ballistocardiography and seismocardiography: A review of recent advances. *IEEE journal of biomedical and health informatics*, 19(4):1414–1427.
- Lee, J., Matsumura, K., Yamakoshi, K.-i., Rolfe, P., Tanaka, S., and Yamakoshi, T. (2013). Comparison between red, green and blue light reflection photoplethysmography for heart rate monitoring during motion. In *2013 35th annual international conference of the IEEE engineering in medicine and biology society (EMBC)*, pages 1724–1727. IEEE.
- Li, S.-H., Lin, B.-S., Wang, C.-A., Yang, C.-T., and Lin, B.-S. (2017). Design of wearable and wireless multi-parameter monitoring system for evaluating cardiopulmonary function. *Medical Engineering & Physics*, 47:144–150.
- Maeda, Y., Sekine, M., and Tamura, T. (2011). Relationship between measurement site and motion artifacts in wearable reflected photoplethysmography. *Journal of medical systems*, 35(5):969–976.
- Pandia, K., Inan, O. T., Kovacs, G. T., and Giovanrandi, L. (2012). Extracting respiratory information from seismocardiogram signals acquired on the chest using a miniature accelerometer. *Physiological measurement*, 33(10):1643.
- Sana, F., Isselbacher, E. M., Singh, J. P., Heist, E. K., Pathik, B., and Armoundas, A. A. (2020). Wearable devices for ambulatory cardiac monitoring: Jacc state-of-the-art review. *Journal of the American College of Cardiology*, 75(13):1582–1592.
- Semiz, B., Carek, A. M., Johnson, J. C., Ahmad, S., Heller, J. A., Vicente, F. G., Caron, S., Hogue, C. W., Etemadi, M., and Inan, O. T. (2020). Non-invasive wearable patch utilizing seismocardiography for perioperative use in surgical patients. *IEEE Journal of Biomedical and Health Informatics*, 25(5):1572–1582.
- Shaffer, F. and Ginsberg, J. P. (2017). An overview of heart rate variability metrics and norms. *Frontiers in Public Health*, 5.
- Shandhi, M. M. H., Semiz, B., Hersek, S., Goller, N., Ayazi, F., and Inan, O. T. (2019). Performance analysis of gyroscope and accelerometer sensors for seismocardiography-based wearable pre-ejection period estimation. *IEEE journal of biomedical and health informatics*, 23(6):2365–2374.
- Tavakolian, K., Portacio, G., Tamddondoust, N. R., Jahns, G., Ngai, B., Dumont, G. A., and Blaber, A. P. (2012). Myocardial contractility: A seismocardiography approach. In *2012 Annual International Conference of the IEEE Engineering in Medicine and Biology Society*, pages 3801–3804. IEEE.
- WHO (2020). The top 10 causes of death. *Geneva: World Health Organization*. <https://www.who.int/news-room/fact-sheets/detail/the-top-10-causes-of-death> (visited: 2022-09).
- Zuckerman, R. B., Sheingold, S. H., Orav, E. J., Ruhter, J., and Epstein, A. M. (2016). Readmissions, observation, and the hospital readmissions reduction program. *New England Journal of Medicine*, 374(16):1543–1551.